

In-situ XAFS Analysis for Fuel Electrode Catalysts of Intermediate Temperature Solid Oxide Fuel Cells

Shigeaki UEMURA*, Junji IIHARA, Aiko TOMINAGA, Yoshihiro SAITO, Chihiro HIRAIWA and Masatoshi MAJIMA

The intermediate temperature solid oxide fuel cell (IT-SOFC) is one of the promising candidates for the clean power supply. In this study, we used the in-situ X-ray absorption fine structure (XAFS) measurement techniques to solve the following two problems in the IT-SOFC development. One is to explore highly active fuel electrode catalysts that dominate the SOFC output power. We measured the reduction rate of the catalysts, since it has a strong correlation with the catalyst activity. Using the simple transmission mode XAFS technique, we evaluated Ni-, Co-, and Fe-based catalysts alone without assembling into SOFC. Our systematic exploration found that annealed pure Ni shows higher reduction rate than Ni alloys. The same trend has been confirmed for Co. In contrast, pure Fe has shown a poorer performance compared to Fe-Ni and Fe-Co alloys. The other problem is to investigate how the support by electrolytes, which is necessary in fabricating SOFC, affects the activity of the catalysts. For this purpose, we also used the in-situ XAFS analyses. Our analyses clarified that the support by electrolytes slightly lowers the activity of pure Ni and Co, whereas it increases the activity of pure Fe.

Keywords: intermediate temperature solid oxide fuel cell, fuel electrode catalyst, in-site XAFS measurement, synchrotron radiation analysis

1. Introduction

Efforts have been under way in recent years to develop clean power generation systems that are free of CO₂ emissions to mitigate global warming. Expectations are growing especially for fuel cells as a home power supply since they emit no CO₂ when they generate power and their generation efficiency is high.

Figure 1 classifies fuel cells by operating temperature and generation efficiency. Among them, the polymer electrolyte fuel cell (PEFC) and the solid oxide fuel cell (SOFC) have come to a more advanced commercial stage than other fuel cells. PEFCs use a proton-conductive solid polymer electrolyte. Although the PEFC requires an expensive platinum catalyst, it has been commercialized as a home or automotive fuel cell system due to its relatively low operating temperature between 80°C and 120°C. Meanwhile, the SOFC uses an

ionically conductive ceramic electrolyte. The advantages of SOFCs include that they can use a less expensive nickel-based catalyst than noble-metal catalysts and that they exhibit high generation efficiency. However, their operating temperature is high between 750°C and 1000°C. Classified as a high-temperature fuel cell, the SOFC has been commercialized as a novel fuel cell for household use.

Compared with PEFCs, high-temperature SOFCs offer higher generation efficiency. However, a drawback to the SOFC is that its cell components are subject to degradation due to its high operating temperature. Accordingly, it has been difficult to reduce the cost of conventional SOFCs due to their need for expensive Inconel and other parts to resist high temperatures.

The present study aims to develop an intermediate-temperature SOFC (IT-SOFC) that operates at a temperature between 400°C and 600°C. In contrast to the use of oxygen ion-conducting electrolyte in high-temperature SOFCs, IT-SOFCs use proton-conductive electrolyte.⁽¹⁾ The IT-SOFC requires neither a platinum catalyst nor a heat-resistant part. Its reduced cost is expected to lead to the wider use of fuel cells.

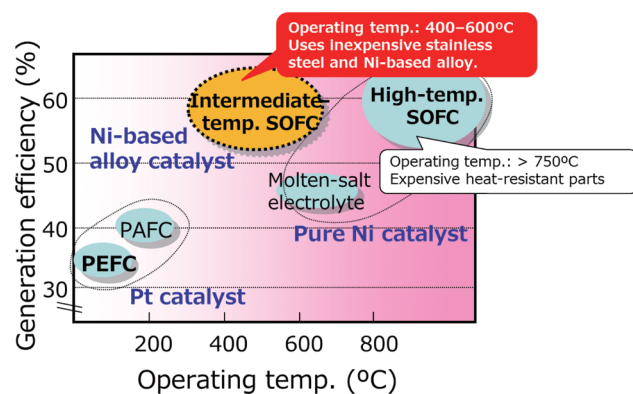


Fig. 1. Fuel cell operating temperature and generation efficiency

2. Finding Solutions to Technical Challenges

Figure 2 shows a model structure and the operating mechanism of the IT-SOFC. In this structure, electrolyte sandwiched between a fuel electrode and an air electrode is located at the center of the cell. Fuel (e.g. hydrogen (H₂) gas) introduced to the fuel electrode side is decomposed by catalytic effect down into protons (H⁺) and electrons. The produced H⁺ moves in the electrolyte and reacts with oxygen at the air electrode to

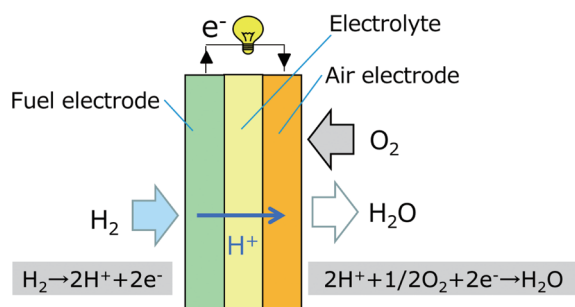


Fig. 2. Structural schematic of IT-SOFC

make water (H₂O). Meanwhile, electrons reach the air electrode side via an external channel. During this process it is possible to produce electrical energy.

One important technical challenge in the development of an IT-SOFC is to find a high-activity catalyst material for the fuel electrode. The fuel electrode catalyst is an important part exerting influences on the basic performance (power output) of the SOFC. While Ni-, Co-, and Fe-based alloys have been thought to be promising, the optimal alloy composition has remained obscure. Another factor possibly affecting the catalytic activity is the need for SOFC electrolyte to support the catalyst.

Conventionally, the only way to evaluate the catalytic activity was to fabricate an SOFC and measure the output. However, this indirect method involves the fabrication of actual SOFCs using many candidates of catalyst materials, possibly requiring enormous amounts of time and labor. Moreover, since factors other than the fuel electrode, such as the air electrode, electrolyte and electrode contact resistance, also affect the output of an SOFC, exclusively evaluating the performance of the fuel electrode has remained a challenge.

As a solution to these two challenges, in the present study, we used synchrotron radiation^{*1} analyses. Saga-LS and other synchrotron radiation facilities enable users to carry out their analysis projects in an extremely short time since such facilities provide higher-intensity X-rays than from commercially available systems by a factor of ×10,000 or more. The X-ray absorption fine structure (XAFS) method^{*2} was used to evaluate the catalytic activity. This technique enables the user to measure changes in the state of catalytic elements in-situ in real time by examining the spectral form near the absorption edge and analyzing the chemical state of the elements in the material.

In-situ XAFS measurement has been reported by many researchers in relation, for example, to lithium ion batteries (LIBs).⁽²⁾ Popular anodes of LIBs are made of oxides of transition metals such as Ni and Co. Studies have been pursued investigating what changes occur in the valence of Ni and other elements in response to Li ions moving in and out during charge and discharge cycles. The fuel electrode catalysts examined in the present study also comprise Ni and other transition metals, as in LIBs. The point is, as stated earlier, the

need for the evaluation of the activity of the catalyst in an unassembled condition rather than that of the entire SOFC.

It was known through our studies that the reduction reactivity of Ni and other catalytic materials is highly correlated with catalytic activity. We had empirically verified that catalytic activity is higher with decreasing reduction temperature in NH₃ atmosphere, as shown in **Figure 3**. Consequently, in-situ measurement of catalytic materials in a reduction atmosphere and evaluating their reduction reactivity was expected to enable the researcher to find high-activity catalysts.

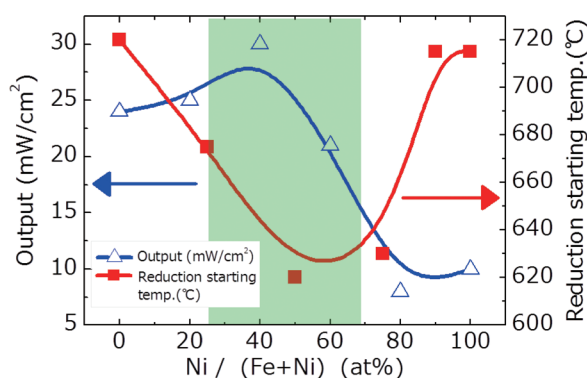


Fig. 3. Relationship between reduction starting temperature of NH₃ decomposing element and power output

For actual in-situ XAFS measurement for catalyst exploration, it would be necessary to optimize conditions such as the concentration of reducing gas and measurement time intervals. It would also be necessary to use a suitable indicator for quantitative comparison of reduction reactivity. These requirements are discussed in detail in the following section.

3. Experiments

3-1 Preparation of fuel electrode samples

Fuel electrode samples were prepared from pure Ni, Co and Fe, as well as from binary and ternary alloys of these metals. This section describes the sample preparation process, taking a ternary Ni-Fe-Co alloy as an example. First, NiO powder is mixed in an aqueous solution of ferric nitrate, and the solution is dried to allow the powder to be impregnated with the solution content. Next, the powder is impregnated with an aqueous solution of cobalt nitrate. Finally, a powder alloy sample is obtained through heat treatment of the powder. **Photo 1** shows an SEM image of the heat-treated powder alloy sample. Other samples were prepared including pure Ni, Co and Fe supported by electrolyte. Yttrium-doped barium zirconate (BaZr_{0.8}Y_{0.2}O_{3-δ}, BZY), which is a typical proton-conductive oxide, was used as the electrolyte. The supported sample was prepared by

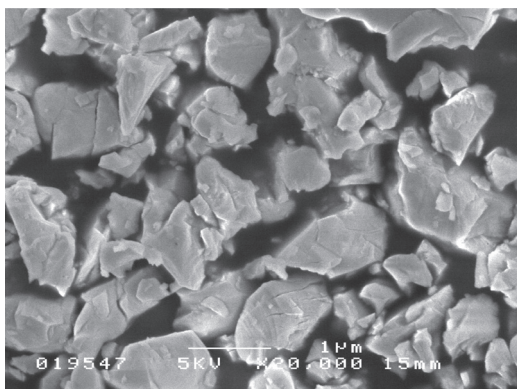


Photo 1. SEM image of heat-treated powder alloy sample

blending oxides, including NiO, and the BZY electrolyte in a mortar, followed by heat treatment.

Each of the above catalysts was tableted (7 mm in diameter and 3 mm in thickness) after being mixed with a diluent (Al₂O₃ and BN) to achieve an optimal absorption coefficient for XAFS measurement. In this process, tablets were hand-compacted (at approx. 0.6 kgf/cm²) in an SUS tube and made porous instead of being tableted by a hydraulic press, in order to ensure the permeation of atmospheric gas and ease of sample handling.

3-2 XAFS measurement

The BL11 of Saga-LS and the BL14B2 of SPring-8 were used to conduct XAFS measurement in transmission mode. **Figure 4** shows the measurement scheme. The above tablet sample held in an SUS tube was secured in a self-made quartz holder, which was then placed in a commercially available heating furnace. The incident X-ray energy was scanned near the K absorption edge of Ni and other elements, and the X-ray intensity before and after transmission through the sample was measured with an ion chamber detector to determine the X-ray absorption spectra.

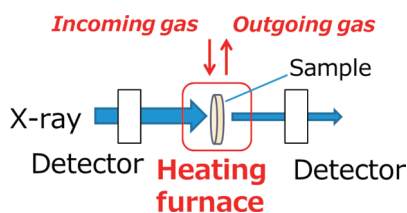


Fig. 4. Outline of transmission XAFS

The catalyst starts reduction reaction when the atmospheric gas is switched from helium (He) to H₂ after a reduction temperature increase up to 400°C. However, exceedingly fast reduction reaction, which occurs in 100% H₂, in 90 s-interval XAFS measurement would fail to make a detailed evaluation of profile

changes since the intermediate state is represented only by one point between the start and end of reaction (**Figure 5 (a)**). As a solution, H₂ diluted with He was used to set conditions. The result was that an H₂ concentration of 10% would enable the evaluation of XAFS profile changes over time in 90 s intervals using the quick scan mode (**Fig. 5 (b)**).⁽³⁾ Incidentally, in successive measurement cycles, measurement required approximately 40 s and data transfer and moving the spectrometer required approximately 50 s. Since the gas was switched at the end of the previous measurement cycle, measurement immediately following a gas change started after a gas flow duration of approximately 50 s. In this report, that measurement is defined as measurement at 0 s following H₂ introduction.

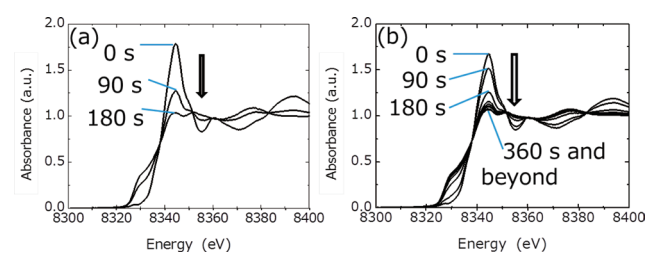


Fig. 5. Hydrogen concentration dependence of changes over time of Ni XAFS at 400°C

3-3 Spectrum analysis and definition of reduction efficiency

Linear combination fitting (LCF) was conducted on spectrum measurements to convert the catalyst reduction state into numbers. For this purpose, the analysis software Iffeffit-Athena⁽⁴⁾ was used.

The analysis involved: XAFS spectrum measurement of Ni metal and NiO, used as a reference sample; taking the sum of the XAFS spectrum measurements multiplied by composition figures; and calculating the sum of squares of the differences between said sum and spectrum measurements of Ni catalyst. This calculation is repeated while fine-tuning the composition figures. Composition figures that minimize the sum of squares of the differences are the composition figures of the catalyst sample. For this calculation, the percentage of the Ni metal in the overall Ni amount is defined as the reduction efficiency and the slope of the reduction efficiency versus time curve is defined as the reduction rate to use as an indicator of reduction reactivity. **Figure 6** shows an example analysis of a Ni catalyst.⁽⁵⁾ In this example, NiO and Ni metal accounted for 48% and 52%, respectively, with the reduction efficiency being 52%. Similar techniques were used to conduct the analysis at the absorption edge of Ni, Co and Fe. Regarding the spectra of the reference samples used in the present study, the Ni-based catalysts were Ni, NiO and NiFe₂O₄, Fe-based catalysts were Fe, Fe₂O₃, Fe₃O₄ and NiFe₂O₄, and Co-based catalysts were Co, CoO and Co₃O₄.

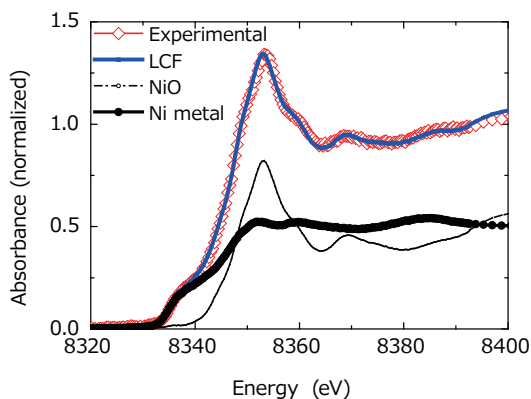


Fig. 6. Linear combination fitting of Ni catalysts 36/ Before He introduction

4. Results and Discussion

4-1 Reduction behavior of unassembled fuel electrode catalysts

As an example of the measurement results, **Figure 7 (a)** shows changes over time of the XAFS spectra of Ni in tertiary alloy $\text{Ni}_{90}\text{Co}_5\text{Fe}_5$ at 400°C .⁽⁶⁾ Before H_2 introduction, the spectra exhibited great similarity with those of NiO. Of note is the intensity of the white line (peak near 8350 eV) specific to Ni oxides. After H_2 introduction, the intensity decreased with time and the curve approaches the spectral form of Ni metal shown in the same figure, indicating a reduction process from oxide to metal. **Fig. 7 (b) and (c)** show spectra of Co and Fe obtained from the same sample. Before H_2 introduction, Co exhibited a highly similar spectral form to that of CoO. After H_2 introduction, the peak intensity at 7728 eV decreased. Exhibiting an isosbestic point by these catalysts, including the Co metal, is interpreted as a progress in reduction from CoO to Co. Meanwhile, in the case of Fe, before H_2 introduction, no catalysts exhibited spectral form conformity with the reference sample. After H_2 introduction, the intensity of the white line (7133 eV) decreased over time and a shift to lower energy occurred at the absorption edge, indicating a progress in reduction. However, the magnitude of the change was small. Consequently, compared with Ni and Co, Fe catalysts obviously tend less to be reduced from oxide to metal.

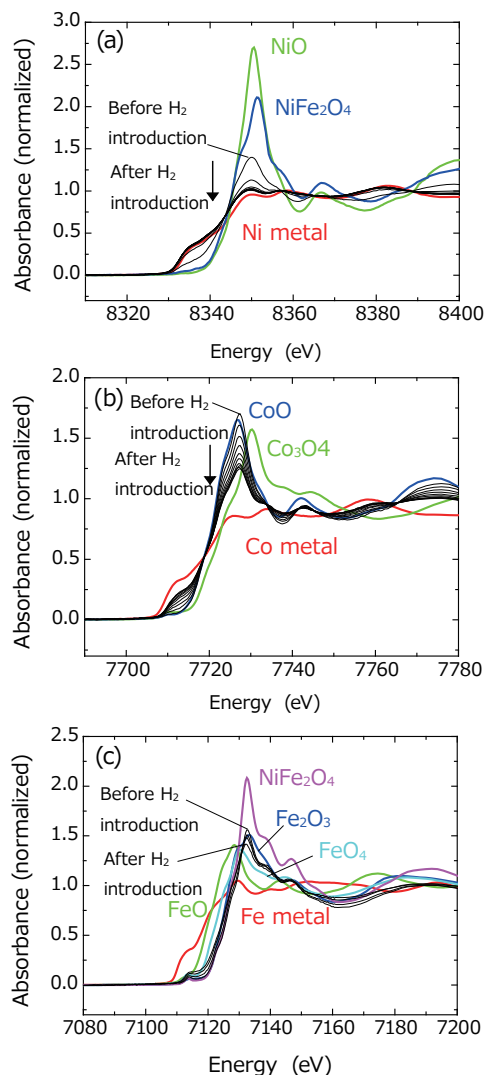


Fig. 7. Changes over time in $\text{Ni}_{90}\text{Co}_5\text{Fe}_5$ XAFS spectra Measurement intervals were 90 s for (a) Ni and (b) Co and 360 s for (c) Fe

Figure 8 compares reduction efficiency obtained through LCF analysis of measurement results of three levels of catalyst samples with different composition ratios. **Fig. 8 (a)** shows results for Ni. The reduction rate

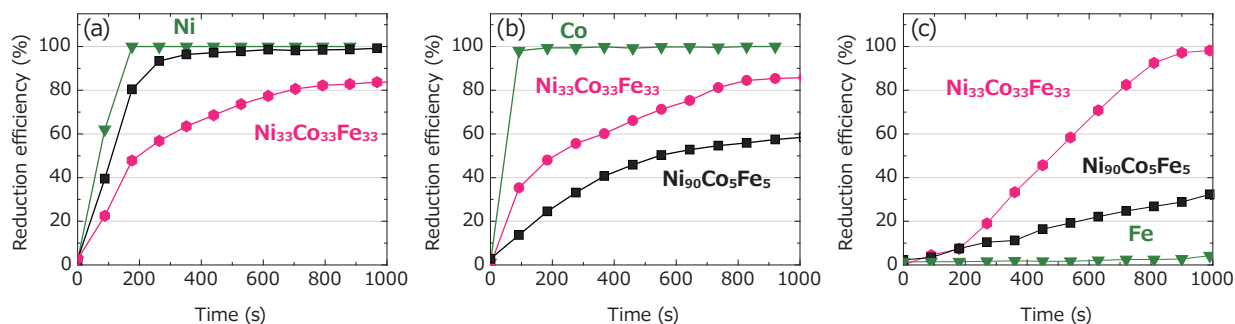


Fig. 8. Time dependence of reduction efficiency of Ni-Fe-Co catalysts and pure metal catalysts for (a)Ni, (b)Co, (c)Ni

is higher with increasing Ni proportion. In addition, the reduction efficiency is high at 900 s after the start of reduction. **Fig. 8 (b)** shows results for Co. Similarly to Ni, the reduction efficiency and the reduction rate are high with increasing proportion of Co. In contrast, while pure Fe barely facilitates reduction, $\text{Ni}_{33}\text{Co}_{33}\text{Fe}_{33}$ and $\text{Ni}_{90}\text{Co}_5\text{Fe}_5$ exhibit an increased reduction rate and efficiency, as shown in **Fig. 8 (c)**. Specifically, Fe in $\text{Ni}_{33}\text{Co}_{33}\text{Fe}_{33}$ is almost 100% reduced, demonstrating the effectiveness of the alloying of Fe.

4-2 Effects of support by electrolyte on changes in reduction behavior

Figure 9 shows different changes over time in reduction efficiency of pure metals observed depending on whether or not they were supported by BZY electrolyte. First, the reduction efficiency of Ni, without support, reached 100% approximately 180 s after H_2 introduction. By contrast, with support by electrolyte, the reduction efficiency was not in excess of 82% and reaching this percentage required 800 s or more. Moreover, the reduction rate rose slowly, approximately 90 s after H_2 introduction.

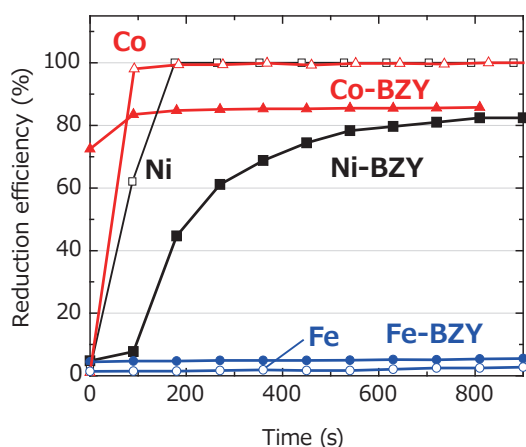


Fig. 9. Time dependence of reduction efficiency of pure-metal catalysts supported by electrolyte

Second, in the case of Co, without support, the reduction efficiency reached almost 100% approximately 90 s after H_2 introduction. With support, the eventual reduction efficiency, 82%, was lower than without support, although it approached 70% immediately after H_2 introduction. These results elucidate the progress of reduction reaction in a very short duration of approximately 50 s between H_2 introduction and the beginning of measurement. Consequently, the effect of support by electrolyte in the case of Co is an increased initial reduction rate and a reduced eventual reduction efficiency.

Finally, for Fe, without support, the reduction efficiency was approximately 3%, which, with support by electrolyte, rose to approximately 6%. However, in either

case, Fe exhibited far lower reduction efficiency than Ni or Co.

4-3 Composition dependence of reduction efficiency

Figure 10 shows an overall graph of reduction efficiency exhibited 900 s after the beginning of reduction, by pure metals and binary and tertiary alloys. The graph reveals that pure Ni and pure Co have the highest catalytic activity among the evaluated materials.

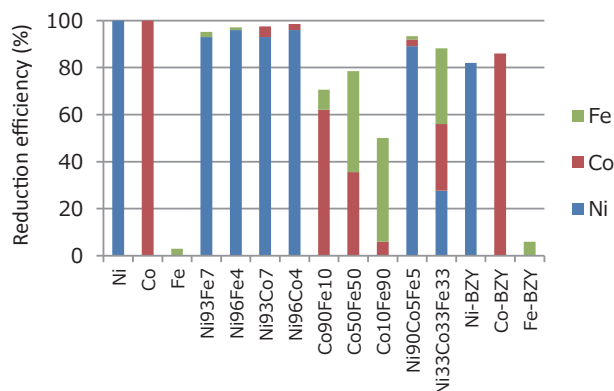


Fig. 10. Composition dependence of reduction efficiency

The results of the experiments are summarized below.

- 1) Alloy composition dependence of reduction efficiency: Alloy < Pure metal for Ni and Co, in contrast to Alloy > Pure metal for Fe
- 2) Effects of support by electrolyte: In the cases of Ni and Co, the eventual reduction efficiency decreases due to support.
- 3) Comparison of metals: The reduction efficiency of Fe is far lower than Ni and Co.

Thus, pure Ni and Co are believed to be the most highly active catalysts among those evaluated in the present study. However, Co-Fe alloy catalysts are also worthy of note. The results suggest that although pure Fe exhibits a very low rate of reduction, once alloyed with Co, the element works as a highly active catalyst with high reduction efficiency. Since this tendency was absent with Ni-Fe alloys, it is believed that the co-presence of Co and Fe leads to the increased reduction efficiency of Fe. The reduction efficiency of Fe was also high in tertiary Ni-Co-Fe alloys, suggesting the apparent effects of Co. While, when supported by BZY, Ni and Co exhibited reduced reduction efficiency, Fe, when supported by BZY, conversely exhibited increased reduction efficiency. Accordingly, it is expected that by using the relationships of Fe and BZY as well as of Co and Fe, it will be possible to create a catalyst with no decrease in reduction efficiency even with support by BZY. Future tasks in our study include focusing on combinations of Ni, Co and Fe with other metals and the catalyst particle size.

5. Conclusion

Two technical challenges encountered in the development of IT-SOFCs were addressed using in-situ XAFS analysis. First, fuel electrode catalysts were explored, using catalyst samples not assembled into an SOFC and conducting in-situ XAFS transmission measurement at 90 s intervals, in a diluted H₂ atmosphere and at 400°C. The obtained data was analyzed by linear combination fitting to calculate reduction efficiency, or reduction rate, which is positively correlated with catalytic activity. The analysis results revealed that pure Ni or Co has higher catalytic activity than Ni- or Co-based alloys, while Fe alloyed with Ni or Co has higher activity than pure Fe.

Next, the activity of catalyst supported by BZY electrolyte was also evaluated through in-situ XAFS measurement. The evaluation results confirmed that when supported by electrolyte, pure Ni and pure Co have reduced activity, while pure Fe conversely exhibits increased activity.

The findings obtained from the in-situ XAFS measurement were applied to fuel cells, whose output improved at operating temperatures below 600°C, especially in the low temperature range. Our future task is to improve the power output of fuel cells by upsizing them and developing them into stacks so as to facilitate the commercialization of intermediate-temperature SOFCs.

6. Acknowledgments

The present study has been pursued with the aid of NEDO's Innovation Promotion Program. The experiments were conducted under task numbers: 1204020AT, Saga-LS Long-Term Trial Use, 1303018A, Advanced and Creative Use of Prefecture-Owned BL (Long-Term), and 2011B1918, SPring-8.

Technical Terms

- *1 Synchrotron Radiation: The electromagnetic waves emitted, in the tangential direction, by charged particles (generally, electrons) when they, moving in a magnetic field nearly at the speed of light, change their direction due to the force of the field. In Japan, experiments using synchrotron radiation can be conducted at synchrotron radiation facilities such as SPring-8, PF, Saga-LS and Aichi SR.
- *2 X-Ray Absorption Fine Structure (XAFS) Method: A technique used to obtain information on the state of electrons, specifically on the unoccupied molecular orbitals, of a material, through observation of the absorption of irradiated X-rays by elements of the material.

References

- (1) C. Hiraiwa et al., J. Am. Ceram. Soc., 96-3 (2013) 879
- (2) I. Nakai et al., J. Solid. State. Chem. 140 (1997) 145
- (3) M. Majima et al., SPring-8 Experiment Summary report 2011B1918
- (4) B. Ravel and M. Newville, J. Synchrotron Rad. 12, pp.537-541 (2005)
- (5) A. Tominaga et al., SAGA-LS Experiment Report 1204020AT (2012)
- (6) S. Uemura et al., SAGA-LS Experiment Report 1303018A (2013)

Contributors (The lead author is indicated by an asterisk (*).)

S. UEMURA*

- Ph. D.
Assistant General Manager, Analysis
Technology Research Center



J. IIHARA

- Ph. D.
Senior Assistant General Manager, Analysis
Technology Research Center



A. TOMINAGA

- Ph. D.
Analysis Technology Research Center



Y. SAITO

- D. Eng.
Group Manager, Analysis Technology
Research Center



C. HIRAIWA

- Assistant Manager, Energy and Electronics
Materials R&D Laboratories



M. MAJIMA

- Ph. D.
Group Manager, Energy and Electronics
Materials R&D Laboratories

